

Simple analytical method for calculating exciton binding energies in semiconductor quantum wells

Henry Mathieu, Pierre Lefebvre, and Philippe Christol

*Groupe d'Etudes des Semiconducteurs, Université de Montpellier II: Sciences et Techniques du Languedoc,
Case Courrier 074, 34095 Montpellier CEDEX 5, France*

(Received 3 February 1992)

We present a very simple method for calculating exciton binding energies in quantum-confined semiconductor structures. The aim of the model calculation, which is developed in the framework of the fractional-dimensional space, is not to compete with the very advanced ones already proposed, but, on the contrary, to avoid tedious and expensive calculations, to obtain, with good accuracy, the exciton binding energy in most of the confined structures where the exciton can be associated with a specific pair of electron and hole subbands. Our main result is an analytical expression for the exciton binding energy, free of any adjustable parameter. Furthermore, in the cases where the $1s$ and $2s$ transition energies can be experimentally measured, the method permits one to obtain the exciton binding energy without any hypothesis or calculation.

I. INTRODUCTION

In recent years there has been considerable interest in the electronic structure, optical properties, and excitons in semiconductor quantum-well structures. These systems display several interesting features, such as the enhancement of optical absorption and emission, which result in well-defined exciton lines, even at room temperature. Clearly, excitons have large effects on optical phenomena observed in these structures, so that an understanding of their properties, such as the increase in binding energy and oscillator strength due to confinement effects, has become an important topic in the physics of multilayer systems.

Following the work of Miller *et al.*,¹ several authors have calculated binding energies of excitons in both infinite¹⁻³ and finite quantum wells.⁴⁻¹¹ All these calculations are variational, including or not different phenomena such as valence-band mixings, nonparabolicity of dispersion relations, effective-mass, and/or dielectric-constant mismatch between the well and barrier materials, Coulomb coupling between excitons belonging to different subbands, etc. These calculations need important computation times and the accuracy of the result depends to a large extent on the form of the trial wave function.

Recently, neglecting valence-band mixings, Leavitt and Little¹² presented a simple method for calculating exciton binding energies in quantum-confined structures. The main result obtained in this paper is an expression for the exciton binding energy as the integral of a prescribed function, using five numerical parameters, weighted by the squares of the electron and hole subband envelope functions. In this approach, because details of the structure are included only through the subband envelope functions, the method can be applied to a wide variety of structures in which the exciton can be associated with a specific pair of electron and hole subbands.

In the present work, we take a step toward the

simplification and generalization. We present a fully analytic method, free of any adjustable parameter. The method uses the model of fractional-dimensional space already employed to study Wannier-Mott excitons in anisotropic solids.¹³ The excitons in an anisotropic solid, like a quantum well, are treated as the ones in an isotropic fractional-dimensional space, where the dimension is determined by the degree of anisotropy. Such a space, termed dynamic space, differs from the one that embeds geometric bodies in that its dimensionality is determined by the physical interactions. Concerning the excitons in quantum-well structure, the question is what is the spatial dimension α which measures the anisotropy of the electron-hole interaction? Knowing α , the model enables one to study exciton binding energy continuously from three-dimensional (3D) to 2D or 1D structures.

The aim of the method proposed here is not to compete with the very advanced ones like the very accurate theory proposed by Andreani and Pasquarello.¹¹ On the contrary, it is to avoid tedious calculations to obtain, with reasonable accuracy, the exciton binding energy in most of the type-I confined structures. In its analytic, very simple form, the method takes into account the effective-mass and dielectric-constant mismatches and the conduction-band nonparabolicity. We obtain a satisfactory agreement with both experimental results and calculations of Andreani and Pasquarello,¹¹ but stay free of tedious computer calculations.

II. MODEL CALCULATION

By using the effective-mass and nondegenerate-band approximations, the relative motion of a free exciton can be described by the Schrödinger equation

$$\left[-\frac{\hbar^2}{2\mu} \nabla^2 - \frac{e^2}{\epsilon r} \right] \psi(r) = (E - E_g) \psi(r), \quad (1)$$

where μ is the electron-hole reduced mass, ϵ is the dielec-

tric constant, r the electron-hole distance, and E_g the energy gap. For an isotropic material, Eq. (1) is similar to the simple hydrogen-atom problem whose solutions are rather straightforward. In an anisotropic system, like layer-type or chainlike materials, an additional anisotropic potential should be added, and the calculation becomes more difficult. In that case a two-dimensional (2D) or one-dimensional (1D) model was generally assumed for the simplicity of the mathematical treatments.

Concerning excitons in semiconductor quantum wells, it is well known that the system is somewhere in between a 2D and a 3D system. Then, neither the 3D nor the 2D model is a good one and a more suitable model is needed to treat the appropriate degree of anisotropy. To date, all the solutions¹⁻¹² except one¹³ use a 3D model, i.e., an isotropic coordinate system with an anisotropic Hamiltonian. However, as these models do not correspond to the real problem, the mathematical solutions are tedious and need numerical calculations with variational or perturbational approach.

The original method proposed by He¹³ consists of stating that, because the real problem is neither purely 3D nor purely 2D, a fractional-dimensional space should be used to simplify the mathematical treatments. In this model, the anisotropic interactions in the 3D space are treated as isotropic ones in a lower fractional-dimensional space, where the dimension α is determined by the degree of anisotropy. In other words, the fractional-dimensional model consists of solving the Schrödinger equation in a noninteger-dimensional space where the interactions actually experience an isotropic environment. In this space the quantum-well exciton problem again comes back to the one of an hydrogen-like atom.

By using this model, He¹³ calculated the exciton bound-state energies and wave functions as a function of spatial dimension α by solving a simple hydrogenic Schrödinger equation in an α D space. The discrete bound-state energies and orbital radii are given by

$$E_n = E_g - \frac{E_0}{\left[n + \frac{\alpha-3}{2} \right]^2}, \quad (2a)$$

$$a_n = a_0 \left[n + \frac{\alpha-3}{2} \right]^2, \quad (2b)$$

where $n = 1, 2, \dots$ is the principal quantum number, E_0 and a_0 are, respectively, the effective Rydberg constant and effective Bohr radius, $E_0 = (\epsilon_0/\epsilon)^2(\mu/m_0)R_H$ and $a_0 = (\epsilon/\epsilon_0)(m_0/\mu)a_H$. R_H and a_H are the Rydberg constant and Bohr radius, respectively. m_0 is the free-electron mass, μ is exciton reduced mass $1/\mu = 1/m_e + 1/m_h$.

According to Eq. (2a), the binding energy of the 1s exciton is given by

$$E_b = \left[\frac{2}{\alpha-1} \right]^2 E_0. \quad (3)$$

$\alpha = 3, 2$, or 1 give, respectively, $E_b = E_0, 4E_0$, or ∞ , corresponding to the well-known results of the integer-

dimension models.

In a real quantum-well structure, α changes continuously between 3 and 2. As the well width decreases, both electron and hole envelope functions become compressed, the Coulomb attraction between the electron and the hole becomes anisotropic and the fractional dimension α decreases from 3 toward 2. For very narrow wells, the envelope functions spread into the barriers, their spatial extents actually begin to increase as the well width decreases. Consequently α does not lead to 2, but has a minimum value corresponding to the onset of this spreading.

Thus the main problem is to define the fractional dimension α , which describes the degree of anisotropy of the electron-hole interaction. This parameter should be related to a quantity which accounts for the spatial extension of this interaction. A possible choice is to express α in terms of the average electron-hole distance in the quantum-confinement direction (z direction). In this way, the pertinent dimensionless parameter may be written as

$$\beta = \left\langle \frac{|z_e - z_h|}{a_0} \right\rangle = \int_{-\infty}^{+\infty} dz_e dz_h \frac{|z_e - z_h|}{a_0} |f_p^e(z_e)|^2 |f_q^h(z_h)|^2, \quad (4)$$

where $f_p^e(z_e)$ [$f_q^h(z_h)$] is the electron (hole) envelope function corresponding to the p th (q th) electron (hole) quantum level. a_0 is the three-dimensional effective Bohr radius. It should be noted that a_0 has been included under the integral sign since, in finite quantum wells, it depends on the distributions of the envelope functions between the well and barrier materials.

Then the fractional dimension α may be related to the reduced average electron-hole distance β by a simple exponential law like

$$\alpha = 3 - e^{-\beta}. \quad (5)$$

$\beta \rightarrow \infty$ corresponds to the three-dimensional case ($\alpha = 3$), $\beta = 0$ corresponds to the two-dimensional case ($\alpha = 2$).

A. Infinite quantum well

Let us consider first the purely academic model of the infinite quantum well. In that case, by taking the center of the well as the zero of the coordinates, the envelope functions are

$$f_p^e(z_e) = \left[\frac{2}{L_w} \right]^{1/2} \sin \left[p \frac{\pi}{L_w} z_e + p \frac{\pi}{2} \right], \quad (6a)$$

$$f_q^h(z_h) = \left[\frac{2}{L_w} \right]^{1/2} \sin \left[q \frac{\pi}{L_w} z_h + q \frac{\pi}{2} \right]. \quad (6b)$$

If the electron and hole quantum wells are infinitely deep, only the excitons corresponding to $p = q$ are allowed.¹⁴ Then by using the envelope functions (6a) and (6b) with $p = q$, Eq. (4) gives

$$\beta = \frac{L_w}{a_0} \left[\frac{1}{3} - \frac{1}{p^2} \frac{5}{4\pi^2} \right], \quad (7)$$

where a_0 is the effective Bohr radius of the three-dimensional exciton within the well material. β varies from about $L_w/5a_0$ for $p=1$ to $L_w/3a_0$ when p goes to the infinity. Now let us consider the ground-state transitions $e1\text{-hh}1$ or $e1\text{-lh}1$. In Fig. 1 we compare our results with those obtained by Bastard *et al.*² from variational calculations. The dimensionless exciton binding energy E_b/E_0 is plotted as a function of the dimensionless well width L_w/a_0 . Clearly, our results obtained by using Eq. (5) to determine the fractional dimension α (curve 2 in Fig. 1) are not in satisfactory agreement with the variational calculations. The reason for this discrepancy probably arises from the fact that the choice of the average electron-hole distance in the z direction as the pertinent parameter to determine the fractional dimension α , is not the best one.

Effectively, a better result is obtained by using as a pertinent parameter the reduced value of the well width L_w , the scaling parameter being the effective Bohr diameter $d_0=2a_0$ of the three-dimensional exciton. The physical meaning of the quantity $L_w/2a_0$ corresponds to the ratio of a length characteristic of the electron and hole motions with regard to the quantum-well effect (L_w), to a length characteristic of the electron-hole relative motion with regard to the Coulomb interaction (d_0). In this way α is given by

$$\alpha = 3 - e^{-L_w/2a_0}. \quad (8)$$

Then, by using Eq. (3) together with Eq. (8), the binding energy of a confined exciton may be written as

$$E_b = \frac{E_0}{\left[1 - \frac{1}{2}e^{-L_w/2a_0}\right]^2}. \quad (9)$$

E_b is the confined exciton binding energy, E_0 and a_0

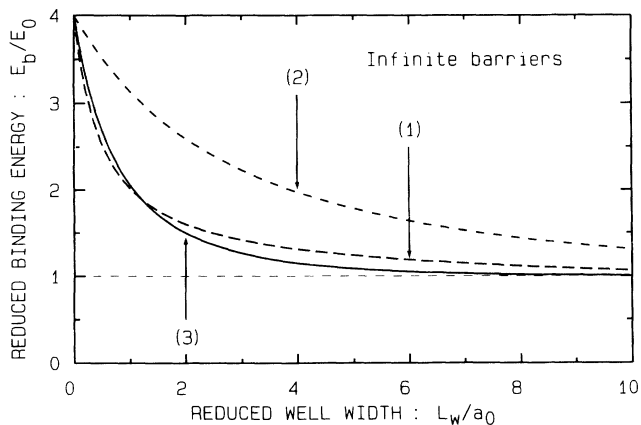


FIG. 1. Dimensionless exciton binding energy E_b/E_0 as a function of the dimensionless well width L_w/a_0 for an infinite quantum well. E_0 and a_0 are the three-dimensional effective Rydberg and Bohr radius, respectively, calculated with the transverse reduced mass. The curve labeled 1 has been obtained by Bastard *et al.* (Ref. 2) from variational calculation (trial wave function ψ_2 in Ref. 2). The curves labeled 2 and 3 correspond to the fractional dimension α given by Eqs. (5) and (8), respectively.

are the effective Rydberg energy and Bohr radius of the three-dimensional exciton in the well material, L_w is the well width. The results, which correspond to the full line in Fig. 1, appear to be in satisfactory agreement with the variational calculations.

The pertinent parameter, which accounts for the relative weights of the quantum-well effect and Coulomb interaction, is written in terms of the electron-hole-pair motion. Alternatively, this parameter may be expressed in terms of the electron-hole-pair energy. Let us define $E_c = E_e + E_h$ as the electron-hole-pair confinement energy, where E_e and E_h are the individual electron and hole confinement energies. A straightforward calculation gives $L_w^2 E_c = h^2/8\mu$, where μ is the electron-hole reduced mass. In a same way the 3D exciton binding energy E_0 is related to the exciton Bohr radius a_0 by the relation $\pi^2 a_0^2 E_0 = h^2/8\mu$. As a result, the physical parameters characteristic of the electron-hole pair with regard to both the quantum-well effect and Coulomb interaction verifies the relation

$$\pi^2 a_0^2 E_0 = L_w^2 E_c. \quad (10)$$

Consequently, E_c is of the order of E_0 when $L_w = 2a_0$. Thus, for narrow wells ($L_w \ll 2a_0$ and then $E_c \gg E_0$) the dominant contribution to the energy of the electron-hole pair is the confinement energy. The resulting electron and hole states are 2D like and the subsequent electron-hole Coulomb interaction gives rise to a 2D-like exciton. On the contrary, for wide wells, the dominant contribution to the electron-hole-pair energy is the Coulomb energy. The resulting state is a 3D exciton possibly perturbed by a one-dimensional potential. In between the two limiting cases the effects compete with one another. Our model consists of calculating the isotropic Coulomb interaction on the basis of the confined states in an αD space.

B. Finite quantum well

In finite quantum wells, it is well known that as the well width decreases below a given value, the envelope functions spread into the barriers. Then, the spreadings of the electron and/or hole inside the barrier material partially restore the three-dimensional character of the exciton. Consequently, the fractional-dimension α does not lead to 2 as the well width becomes very small, but should come back to 3 and must be expressed as a function of this spreading.

Let us briefly recall the one-dimensional motion of a particle (electron or hole), of effective mass m , in a square quantum well characterized by a well depth V and a well width L_w . By taking the bottom of the well as the zero of the energy, the bound-state energies E_p of the particle are given by the well-known transcendental equation which may be written

$$k_w L_w = p\pi - 2 \arcsin \left(\frac{k_w/m_w}{\sqrt{k_w^2/m_w^2 + k_b^2/m_b^2}} \right) \quad (11)$$

where the characteristic wave vectors k_w and k_b are given by

$$k_w = \frac{\sqrt{2m_w E_p}}{\hbar}, \tag{12a}$$

$$k_b = \frac{\sqrt{2m_b (V - E_p)}}{\hbar}. \tag{12b}$$

m_w and m_b are the effective masses of the particle in the well and barrier materials, respectively.

Inside and outside the quantum well, the z motion of the particle is described by the respective envelope functions

$$\xi_w(z) = A \sin(k_w z + \varphi), \tag{13a}$$

$$\xi_b(z) = B e^{\pm k_b z}. \tag{13b}$$

In the infinite quantum well, the dimensionless pertinent parameter used to characterize the electron-hole interaction was the reduced well width, defined as $L_w/2a_0$. In a same way, in a finite quantum well, the pertinent parameter may be written as $L_w^*/2a_0^*$, where L_w^* and a_0^* have the corresponding meanings in the finite well.

L_w^* should represent the spatial extension of the particle motion in the z direction; then, taking into account the spreading into the barriers on both sides of the well, L_w^* may be written as

$$L_w^* = \frac{1}{k_b} + L_w + \frac{1}{k_b}, \tag{14}$$

where k_b is given by the solution of Eq. (11). Now, concerning the electron-hole pair, the electron and hole spreadings into the barriers are to be combined to define a length characteristic of the z motion of the electron-hole pair. Here the question is when the electron and hole spreadings are very different, which of the two carriers rules the pair motion with regard to the well potential? Before answering that question, we note that, with regard to the only square-well potential, there is no electron-hole interaction to take into account. As a result, when the electron and hole spreadings are very different, the more delocalized particle partially restores a three-dimensional character to the electron-hole distance, or equivalently, to the center-of-mass motion. Consequently, the spreading of the pair into the barriers may be written as

$$\frac{1}{k_b} = \frac{1}{k_{be}} + \frac{1}{k_{bh}}, \tag{15}$$

where k_{be} and k_{bh} are given by the solution of Eq. (11) for the electron and the hole, respectively. The characteristic length of the motion of the electron-hole pair with regard to the quantum-well effect will be written

$$L_w^* = \frac{2}{k_b} + L_w. \tag{16}$$

Concerning the length characteristic of the Coulomb interaction, we note that the three-dimensional effective Bohr radius a_0 varies with the position-dependent effective masses and dielectric constant. In order to account for the effective-mass mismatch between the well

and barrier materials, let us define two weighting parameters β_e and β_h as

$$\beta_e = L_w / (2/k_{be} + L_w), \tag{17a}$$

$$\beta_h = L_w / (2/k_{bh} + L_w). \tag{17b}$$

By using these parameters, mean values for the electron effective-mass and valence-band parameters can be defined. They are

$$m_e^* = \beta_e m_{ew} + (1 - \beta_e) m_{eb}, \tag{18a}$$

$$\gamma_1^* = \beta_h \gamma_{1w} + (1 - \beta_h) \gamma_{1b}, \tag{18b}$$

$$\gamma_2^* = \beta_h \gamma_{2w} + (1 - \beta_h) \gamma_{2b}. \tag{18c}$$

Then, the mean value of the three-dimensional Bohr radius which is the length characteristic of the Coulomb interaction may be written

$$a_0^* = \frac{\epsilon}{\epsilon_0} \frac{m_0}{\mu^*} a_H, \tag{19}$$

where μ^* is a mean value of the three-dimensional reduced mass of the exciton, which is given by¹⁵ $1/\mu^* \simeq 1/m_e^* + \gamma_1^*$.

The dimensionless pertinent parameter for the finite quantum well is then given by $L_w^*/2a_0^*$ and the fractional dimension α is

$$\alpha = 3 - e^{-L_w^*/2a_0^*} = 3 - e^{-(2/k_b + L_w)/2a_0^*}. \tag{20}$$

The infinite well corresponds to $1/k_b = 0$ and $a_0^* = a_0$, in which case Eq. (20) reduces to Eq. (8). Figure 2 shows the well-width dependence of the fractional dimension α for the heavy-hole exciton in $\text{Ga}_{1-x}\text{Al}_x\text{As}/\text{GaAs}$ quantum wells for different aluminum contents. The minimum value of the fractional dimension varies from $\alpha \simeq 2.2$ for $x = 1$, where the electron and hole well depths are $V_e \simeq 800$ meV and $V_h \simeq 440$ meV, respectively, to $\alpha \simeq 2.5$ for $x = 0.1$, where the electron and hole well depths are $V_e \simeq 80$ meV and $V_h = 44$ meV, respectively.

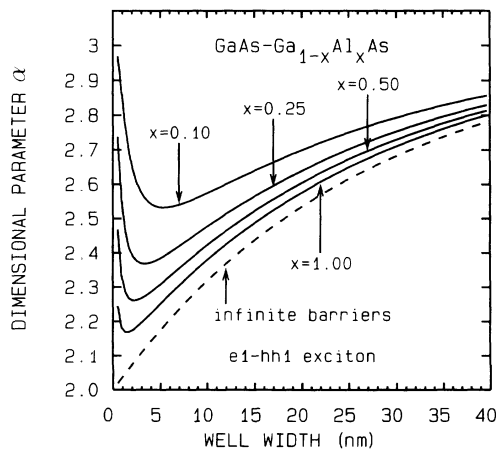


FIG. 2. Well-width dependence of the fractional dimension α . The dotted line corresponds to an infinite well depth. Full lines correspond to $\text{Ga}_{1-x}\text{Al}_x\text{As}/\text{GaAs}$ quantum wells for different values of aluminum content.

On the other hand, the minimum of α is located between $L_w \simeq 20$ Å and $L_w \simeq 50$ Å, corresponding to the well widths giving rise to the maximum binding energy for the corresponding exciton.

By using Eq. (3) together with Eq. (20), we are able to propose a very simple law to obtain the binding energy of the confined exciton in a finite quantum well, without any adjustable parameter:

$$E_b = \frac{E_0^*}{\left[1 - \frac{1}{2}e^{-(2/k_b + L_w)/2a_0^*}\right]^2}, \quad (21)$$

where E_0^* is the mean value of the effective Rydberg energy for the three-dimensional exciton. Now, in bulk zincblende-type semiconductors, the top most valence band is fourfold degenerate and E_0^* may be obtained by using $m_h = 1/\gamma_1$ as a mean value of the hole masses; γ_2 , which describes the effect of the anisotropy, produces small corrections which have been considered in a second-order perturbation theory.¹⁵ On the contrary, in a two-dimensional system the anisotropy is stronger, the heavy- and light-hole subbands are split and the in-plane effective masses are given by $1/m_{hh} = \gamma_1 + \gamma_2$ and $1/m_{lh} = \gamma_1 - \gamma_2$ for the “heavy” and “light” hole, respectively. These in-plane masses, which are relevant for a true two-dimensional exciton, have been used in early calculations (e.g., Ref. 4). This is equivalent to neglecting the off-diagonal terms in the Luttinger Hamiltonian. In more recent approaches (e.g., Ref. 11), the full Hamiltonian was used. Then, the in-plane masses of some subbands can be negative for small k . In the present analytical model, however, it seems very difficult to include more accurate subband dispersions. Instead, we propose an alternative method: considering an α -dimensional system we can use an interpolation in between the two limiting cases. Then, in order to take into account both the spreading of the wave functions into the barriers and the α dependent in-plane effective masses, E_0^* in Eq. (21) is calculated by using the following expressions for the reduced masses:

$$1/\mu_{hh}^* = 1/m_e^* + \gamma_1^* + (3-\alpha)\gamma_2^*, \quad (22a)$$

$$1/\mu_{lh}^* = 1/m_e^* + \gamma_1^* - (3-\alpha)\gamma_2^*, \quad (22b)$$

where m_e^* , γ_1^* , and γ_2^* are given by Eqs. (18).

Equation (21) permits us to calculate the exciton binding energy for different pairs of confined states e_p - h_p , after calculation of the energies of the corresponding electron and hole states given by Eq. (11). Moreover, with α given by Eq. (20), it is possible to calculate the excited-state energies of the exciton ($n \geq 1$) by using Eq. (2a). It must be noted that the light- and heavy-hole exciton binding energies converge to the same value as the well width becomes very large. This results from the α -dependent in-plane reduced masses given by Eqs. (22).

As an application, let us consider the electron heavy-hole $e1$ - $hh1$ and light-hole $e1$ - $lh1$ ground-state transitions. As shown above, the spatial extension $(k_b)^{-1}$ is a crucial ingredient of the calculation. The value of k_b can be extracted from the resolution of Eq. (11), which pro-

vides the values of the confinement energies of the $e1$ electron and $hh1$ ($lh1$) hole. In Appendix A, we propose a very convenient and widely sufficient approximate resolution. This method allows us to obtain a fully analytical method for computing the binding energies of the ground-state excitons, by direct application of Eq. (21). Now, as demonstrated below, the accuracy of this method can even be improved, on the condition that the correct physical ingredients are included.

III. CONDUCTION-BAND NONPARABOLICITY AND DIELECTRIC-CONSTANT MISMATCH

For relatively thin wells, the confinement energies of the electrons become very important and the subbands are fairly far from the bulk band edge. Then the conduction-band nonparabolicity should be taken into account. A convenient way to include this effect in our analytical approach is to express it in terms of energy-dependent effective mass. From recent calculations, Ekenberg¹⁶ shows that the in-plane curvature of the dispersion relation at the bottom of the subband does not correspond to the same effective mass as in the bulk. Furthermore, the anisotropy of the bulk conduction band is found to have larger effect in quantum wells than in the bulk. Relative to the bulk mass, the enhancement of the in-plane mass which is relevant for the calculation of the exciton binding energy is found to be three times stronger than the z -parallel mass which gives the confinement energies. For both infinite and finite quantum wells and both ground and excited states, Ekenberg shows that the energy-dependent effective masses can be written in a very simple form as a function of the confinement energy,

$$m_z \simeq m_e(1 + \alpha'E), \quad (23a)$$

$$m_{\parallel} \simeq m_e[1 + (2\alpha' + \beta')E], \quad (23b)$$

where $\alpha' = -(2m_e/\hbar^2)^2\alpha_0$ and $\beta' = -(2m_e/\hbar^2)^2\beta_0$. Here m_e is the band-edge effective mass in the bulk material and E is the confinement energy. The parameters α_0 and β_0 , which are negative, are determined from a $\mathbf{k}\cdot\mathbf{p}$ calculation.¹⁷ Equation (23b) can be used to calculate the electron effective masses m_{ew} and m_{eb} which appear in Eq. (18a),

$$m_{ew} \simeq m_{ew0}[1 + (2\alpha' + \beta')E_p], \quad (24a)$$

$$m_{eb} \simeq m_{eb0}[1 + (2\alpha' + \beta')(V_e - E_p)]. \quad (24b)$$

m_{ew0} and m_{eb0} are the band-edge effective masses in the well and barrier materials. V_e is the electron quantum-well depth, E_p is the confinement energy. For GaAs, $\alpha' = 0.64 \text{ eV}^{-1}$ and $\beta' = 0.70 \text{ eV}^{-1}$,¹⁵ and we assume that the same values can be used for the barrier material.

Let us now consider the effects of the difference in dielectric constants between well and barrier materials. There are two effects, the first one depending on the amount of the exciton wave function in the barriers, the second one on the strength and position of the image charges. As generally the dielectric constant in the barrier is smaller than in the well, the result is an increase of the exciton binding energy. These effects can be included

in our model calculation in an analytical way. The first one can be taken into account in the calculation of the mean values of the effective Rydberg (E_0^*) and Bohr radius (a_0^*), which appear in Eq. (21). In this way, a mean value of the dielectric constant can be defined as

$$\epsilon^* = \sqrt{\beta_e \beta_h} \epsilon_w + (1 - \sqrt{\beta_e \beta_h}) \epsilon_b, \quad (25)$$

where β_e and β_h are the weighting parameters defined in Eqs. (17a) and (17b).

The effect of the image charges, which is a purely electrostatic one, is very complicated because there are infinite series of image charges associated with the electron and hole motions. Moreover, in finite quantum wells there are four different configurations corresponding to the electron and/or hole inside the well or barrier material. In their accurate calculation, Andreani and Pasquarello¹¹ included this effect by considering an infinite series of image charges. On the other hand, in the limit of infinite barrier, Whittaker and Elliott¹⁸ obtained an estimation of the effect by treating analytically the potential of the first image charge in first-order perturbation theory. The results are fairly close to one another. The perturbation approach yields, for the increase of the exciton binding energy, the following expression:¹¹

$$\Delta E = 2 \frac{\epsilon_w - \epsilon_b}{\epsilon_w + \epsilon_b} \frac{e^2}{\epsilon_w a_0} \frac{I(L_w/a_0)}{L_w/a_0}, \quad (26)$$

where a_0 is the exciton Bohr radius, and

$$I(L_w/a_0) = \int_0^\infty \frac{(2L_w/a_0)^3}{[x^2 + (2L_w/a_0)^2]^{3/2}} \frac{e^{-x}}{[1 + (x/2\pi)^2]^2} \times \left[\frac{\sinh(x/2)}{x/2} \right]^2 dx. \quad (27)$$

The dimensionless quantity $I(L_w/a_0)/(L_w/a_0)$ may be estimated with good accuracy by an analytical expression; then by taking a_0^* in place of a_0 for the finite quantum well, ΔE may be written as

$$\Delta E \approx 2 \frac{\epsilon_w - \epsilon_b}{\epsilon_w + \epsilon_b} \frac{e^2}{\epsilon_w L_w} [1 - e^{-1.7L_w/a_0^*}]. \quad (28)$$

ΔE , which is proportional to the dielectric-constant mismatch, increases as the well width decreases and may be of the order of several meV for narrow wells. For a 50-Å-wide GaAs/AlAs quantum well, Eq. (28) gives $\Delta E \approx 2$ meV.

IV. COMPARISON WITH RECENT THEORETICAL WORKS

As a check on the accuracy of our analytical method, we have calculated the binding energy of the ground-state heavy- and light-hole excitons in different $\text{Ga}_{1-x}\text{Al}_x\text{As}$ -GaAs quantum wells as a function of the well width. In order to compare our results with those of different numerical calculations, we have used, in each case, the same parameters and hypotheses as the corresponding authors. The parameters are the dielectric constant and effective masses inside and outside the well, and the conduction-to valence-band offset ratio. The basic hypotheses differ, from one author to the other, by the inclusion of effects such as the mismatch of the effective masses and/or the dielectric constants between well and barrier materials, or the nonparabolicities of the valence and conduction bands.

Figures 3, 4, and 5 show that the overall trends in our calculations are correct. Binding energies first increase as

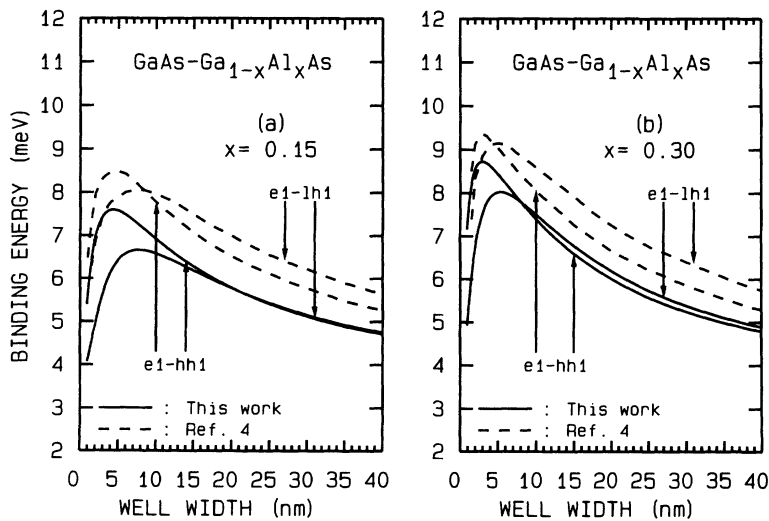


FIG. 3. Binding energies for the heavy- and light-hole excitons in the $\text{Ga}_{1-x}\text{Al}_x\text{As}/\text{GaAs}$ quantum well as a function of the well width. The dashed curves are from Greene *et al.* (Ref. 4). The solid curves were calculated with our model by using the parameter values given in Ref. 4 (a) $x=0.15$, (b) $x=0.30$.

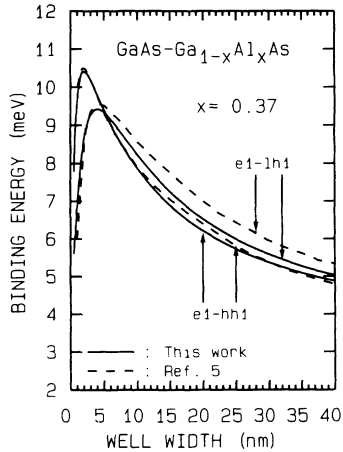


FIG. 4. Same as Fig. 3, where the dashed curves are from Priester, Allan, and Lannoo (Ref. 5).

the well width is reduced, as long as the exciton wave function remains confined in the well region. For narrow wells and finite barrier height, the wave function starts to leak into the barrier material and the binding energies actually begin to decrease toward the corresponding value in the bulk barrier material. As long as the holes are confined inside the well, the heavy-hole exciton binding energy is smaller than the light-hole one because of the ratio of the in-plane effective masses. Nevertheless, on account of the z -direction effective masses, the heavy-hole exciton binding energy begins to decrease later as the well width decreases. We note that, on account of the α -dependent in-plane masses of the holes [Eqs. (22a) and

(22b)], the binding energies of the light- and heavy-hole excitons converge to a same value, corresponding to the 3D exciton, as the well width becomes very large or very small. This is one fundamental difference from all the other calculations for which the binding energies of the light- and heavy-hole excitons tend toward two different values for infinitely wide wells.

In Figs. 3(a) and 3(b), we compare our results with those of Greene, Bajaj, and Phelps.⁴ These authors have calculated the exciton binding energies for the heavy- and light-hole excitons in a quantum-well structure consisting of a single slab of GaAs sandwiched between two semi-infinite layers of $\text{Ga}_{1-x}\text{Al}_x\text{As}$, with $x=0.15$ and 0.30 . They have used a flexible form for the exciton envelope function with several variational parameters, with the same values for effective-mass parameters and dielectric constants in the well and barrier materials. The dispersion relations were taken parabolic. The well width corresponding to the maximum binding energy is exactly the same in our results as in those of Greene, Bajaj, and Phelps,⁴ for both light- and heavy-hole excitons. Concerning the value of the energy, the discrepancy appears to be nearly constant with a typical value of about 1 meV.

In Fig. 4 our results are compared with those of Priester, Allan, and Lannoo.⁵ Here the exciton envelope function chosen by the authors is a simple exponential function of the radial coordinate, but the effective-mass mismatch between the well and barrier materials is taken into account. The bands are parabolic. The agreement is excellent for the heavy-hole exciton and very good for the light-hole one, with a maximum discrepancy lower than 0.5 meV.

In Figs. 5(a), 5(b), and 5(c), we compare our results

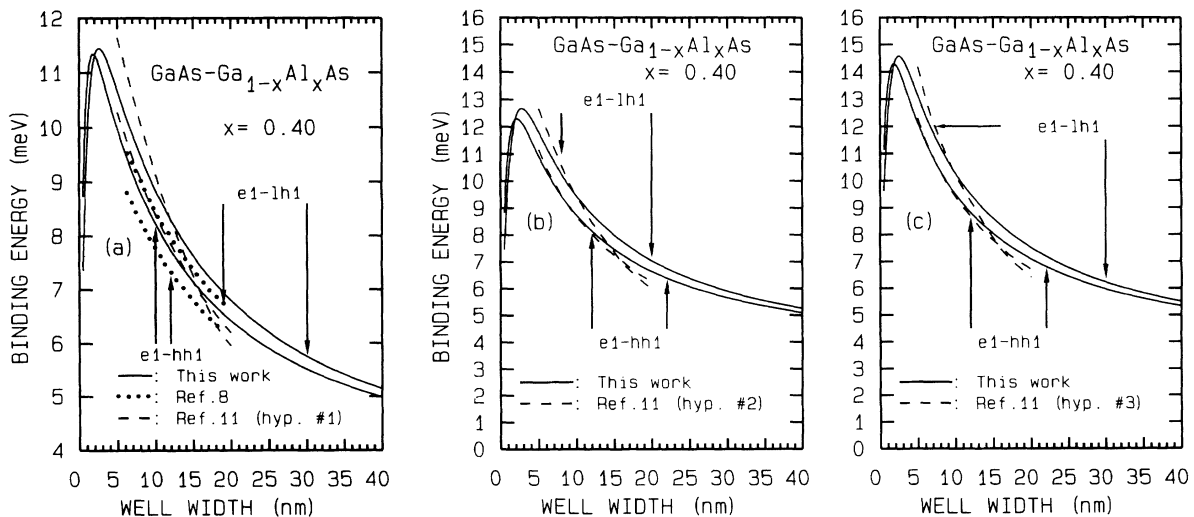


FIG. 5. Binding energies for the heavy-hole and light-hole excitons in the $\text{Ga}_{1-x}\text{Al}_x\text{As}/\text{GaAs}$ quantum well as a function of the well width, for different approximations. Solid lines were calculated with our model. The dashed lines are from Andreani and Pasquarello (Ref. 11). The dotted lines in (a) are from Ekenberg and Altarelli (Ref. 8). (a) Two-band approximation, parabolic conduction band, equal dielectric constants (hypothesis 1). (b) Including conduction-band nonparabolicity (hypothesis 2), (c) Including both conduction-band nonparabolicity and dielectric-constant mismatch (hypothesis 3).

with the corresponding ones obtained by Andreani and Pasquarello¹¹ as a function of the approximation used in the calculation. Figure 5(a) represents the results obtained in a two-band approximation, with a parabolic conduction band, and using the same value for the well and barrier dielectric constant. Also plotted in the figure are the results obtained by Ekenberg and Altarelli⁸ in their parabolic approximation, using exactly the same parameters. Figure 5(b) includes conduction-band nonparabolicity. Figure 5(c) also includes the dielectric mismatch. The agreement is very good for both the light- and heavy-hole excitons in each approximation. In the parabolic approximation in particular [Fig. 5(a)], our results appear in between those obtained by Andreani and Pasquarello and Ekenberg and Altarelli. Figures 5(a), 5(b), and 5(c) clearly show a regular increase of the maximum value of the binding energies, which vary from 10 meV in the parabolic approximation to 15 meV when the conduction-band nonparabolicity and dielectric mismatch are taken into account.

The results of our calculation were also compared to those of other authors,¹⁹ who used a somewhat different set of hypotheses and parameters. The comparisons are not presented via a figure, for the sake of simplicity, but the difference between both calculations, using the same set, is always much lower than 0.5 meV, for GaAs-Ga_{0.6}Al_{0.4}As quantum wells.

In their accurate calculation, Andreani and Pasquarello also included valence-band mixings and Coulomb coupling between excitons belonging to different subbands. In particular they showed that the effect of Coulomb coupling may be important, especially for the light-hole exciton, increasing the binding energy by more than 2 meV. Clearly these effects cannot be included in an analytical way in our calculation.

As an illustration, Fig. 6 displays the result obtained from our calculation, using the same parameters and hy-

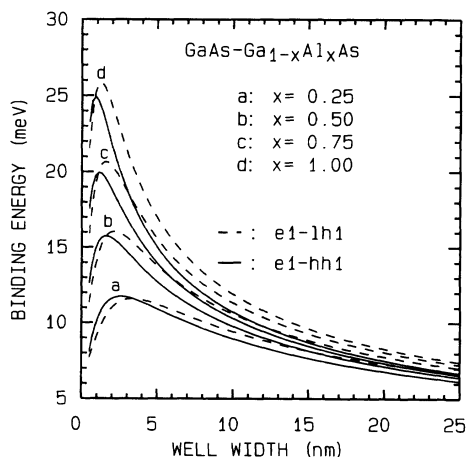


FIG. 6. Example of the calculation of the binding energies of the $1s$ $e1$ - $hh1$ (solid lines) and $e1$ - $lh1$ (dashed lines) excitons in GaAs-Ga_{1-x}Al_xAs quantum wells of varying width and depth, at the Γ point. For high aluminum concentrations and for thin wells, type-II excitons involving X -like conduction states may be observed in photoluminescence. They are not investigated here. Nevertheless Γ -like excitons can still be observed by photoluminescence excitation in the same conditions.

potheses as in Fig. 5(c), but with the energy gap of Ga_{1-x}Al_xAs given by the quadratic law of Bosio *et al.*²⁰

V. COMPARISON WITH EXPERIMENTAL RESULTS

Concerning experimental results, the most reliable measurements come from low-temperature photoluminescence experiments, where a well-defined peak identified as the $2s$ exciton state has been reported. In Fig. 7, we compare some experimental values^{1,21-24} of the energy difference $E_{2s} - E_{1s}$, obtained on several Ga_{1-x}Al_xAs-GaAs quantum wells ($0.31 < x < 0.37$), with our calculation by taking $x = 0.35$. We have chosen the same parameters as for Fig. 6.

Our results are in very good agreement with the experimental ones. The overall trends are correct but the $1s$ - $2s$ splitting energy for the light-hole exciton appears to be smaller than the measured values. This small discrepancy results from the fact that our two-band calculation does not take into account the valence-band mixings and Coulomb coupling between excitons belonging to different subbands. It is well known that, because of mixings which appear at finite values of the in-plane k vector, the in-plane dispersion relations of the hole subbands are nonparabolic, especially for the light holes. Some subbands even have electronlike masses at $k = 0$, increasing both the joint density of states and reduced masses. Exciton binding energies and oscillator strengths, especially for the light-hole excitons, are then increased. This means that, in any equivalent two-band model of the exciton, a value of the in-plane light-hole mass larger than the value at $k = 0$, should be more appropriate. In this way, a mean value calculated over a k extension of the or-

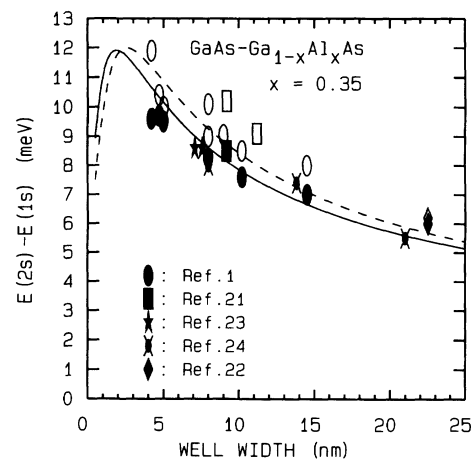


FIG. 7. Comparison of calculated and measured values of the energy difference $E_{2s} - E_{1s}$ for Ga_{1-x}Al_xAs/GaAs quantum wells. Calculated values have been obtained with $x = 0.35$ and the same values of basic parameters as for Fig. 6. Experimental points correspond to $x = 0.31$ and 0.33 (Ref. 24), $x = 0.33$ (Ref. 25), $x = 0.35$ (Refs. 21 and 22), and $x = 0.37$ (Ref. 1). Heavy-hole excitons are represented by full figures, while open figures were used for light-hole excitons. The horizontal size of each point correspond to an uncertainty of ± 1 monolayer in well width. A reasonable value of ± 0.35 meV was taken as an average uncertainty on the value of $E_{2s} - E_{1s}$.

der of $1/a_0$, where a_0 is the three-dimensional effective Bohr radius of the exciton, may be used. In that case a previous calculation of the in-plane dispersion relations of the hole subbands is required.

Finally, one should notice that, from the experimental measurement of the $1s-2s$ splitting energy, it is not easy to obtain the exciton binding energy E_b directly, without either tedious calculation or rough hypothesis such as a purely 3D-like or 2D-like behavior of the exciton. Following the model calculation given above, it is possible to obtain E_b from $E_{2s}-E_{1s}$ in a very simple way. Equation (2a) permits the energy difference $E_{2s}-E_{1s}$ as a function of the fractional dimension α to be expressed, that is

$$\frac{E_{2s}-E_{1s}}{E_0} = \frac{16\alpha}{(\alpha^2-1)^2}. \quad (29)$$

$\alpha=3$ gives the well-known value $(E_{2s}-E_{1s})/E_0 = \frac{3}{4}$, which corresponds to the three-dimensional exciton. $\alpha=2$ corresponds to the two-dimensional exciton for which Eq. (29) gives $(E_{2s}-E_{1s})/E_0 = \frac{32}{9}$; now in that case the exciton binding energy is $E_b=4E_0$, so that we obtain the well-known relation for the 2D exciton $(E_{2s}-E_{1s})/E_b = \frac{8}{9}$. $\alpha=1$ corresponds to the one-dimensional exciton, for which $E_b \rightarrow \infty$.

Equation (29) permits us to obtain the fractional dimension α from the $1s-2s$ splitting energy. It is then possible to calculate E_b from Eq. (3). Figure 8 represents the variation of E_b/E_0 as a function of $(E_{2s}-E_{1s})/E_0$ in the range $2 < \alpha < 3$. Clearly, the dots which represent the values obtained from Eqs. (29) and (3) appear to follow a nearly linear law. Consequently the exciton binding energy E_b may be expressed as a function of the $1s-2s$ splitting energy by a linear relation like

$$\frac{E_b}{E_0} \simeq \frac{108}{101} \frac{E_{2s}-E_{1s}}{E_0} + \frac{20}{101}. \quad (30)$$

Equation (30) corresponds to the full line in Fig. 8.

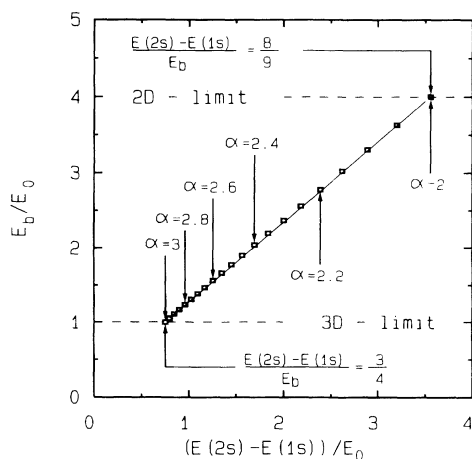


FIG. 8. Dimensionless binding energy of the exciton E_b/E_0 as a function the dimensionless energy difference between $1s$ and $2s$ exciton states, $(E_{2s}-E_{1s})/E_b$. The square dots correspond to the exact values calculated with Eqs. (29) and (3). Full line corresponds to the linear approximation given by Eq. (30).

It is then possible to obtain E_b from $E_{2s}-E_{1s}$ in a very simple and accurate way, without any calculation or hypothesis.

VI. CONCLUSION

We have presented a very simple method for calculating exciton binding energies in quantum-confined semiconductor structures. Our main result is an analytical expression, for the binding energy, free of any adjustable parameter. The method permits one to obtain the exciton binding energy with a reasonable accuracy in most of the confined structures, where the exciton can be associated with a specific pair of electron and hole subbands. Moreover, in the cases where the $1s$ and $2s$ transition energies have been experimentally determined, the method permits one to obtain the exciton binding energy E_b without any hypothesis nor calculation.

Lastly, because of its generality, the method may be extended for calculating exciton binding energies in complex confined structures such as superlattices, quantum wires, or quantum dots. In each case, the problem is to define the fractional dimension α , which describes the degree of anisotropy of the electron-hole interaction. This parameter should be related to a quantity which accounts for the spatial extension of this interaction. In a quantum well α has been related, via Eq. (20), to the ratio of a length characteristic of the electron and hole motions with regard to the quantum-confinement effect (L_w^*), to a length characteristic of the electron-hole relative motion with regard to the Coulomb interaction (a_0^*). In superlattices, as an example, the choice should be different. In that case, the pertinent parameter may be related to the well width and barrier thickness, and/or to the miniband width, and/or to the transverse effective masses.²⁵

APPENDIX A: APPROXIMATE CALCULATION OF THE FIRST CONFINED LEVEL IN QUANTUM WELLS

If we assume the same value for the effective masses in the well and barrier materials, an expansion of Eq. (11) gives rise to an analytical solution. Indeed, assuming $p=1$ and $m_w=m_b=m$, Eq. (11) may be written

$$\sqrt{E/V} = \sin \frac{\pi}{2} (1 - \sqrt{E/E_i}), \quad (A1)$$

where $E_i = \pi^2 \hbar^2 / 2mL_w^2$ is the confinement energy in the corresponding infinite quantum well. On account of the relation $E/E_i < 1$, the sine function may be expanded with a good approximation and Eq. (A1) becomes

$$\begin{aligned} \sqrt{E/V} \simeq & \frac{\pi}{2} (1 - \sqrt{E/E_i}) - \frac{1}{3!} \left[\frac{\pi}{2} (1 - \sqrt{E/E_i}) \right]^3 \\ & + \frac{1}{5!} \left[\frac{\pi}{2} (1 - \sqrt{E/E_i}) \right]^5 \\ & - \frac{1}{7!} \left[\frac{\pi}{2} (1 - \sqrt{E/E_i}) \right]^7. \end{aligned} \quad (A2)$$

Now an expansion of Eq. (A2) to second order gives

$$E + \left[\frac{B}{C} \sqrt{E_i} - \frac{1}{C} \frac{E_i}{\sqrt{V}} \right] \sqrt{E} + \frac{A}{C} E_i \approx 0 \quad (\text{A3})$$

with

$$A = \frac{\pi}{2} - \frac{1}{3!} \left[\frac{\pi}{2} \right]^3 + \frac{1}{5!} \left[\frac{\pi}{2} \right]^5 - \frac{1}{7!} \left[\frac{\pi}{2} \right]^7 = 0.9998 \approx 1, \quad (\text{A4a})$$

$$B = -\frac{\pi}{2} + \frac{3}{3!} \left[\frac{\pi}{2} \right]^3 - \frac{5}{5!} \left[\frac{\pi}{2} \right]^5 + \frac{7}{7!} \left[\frac{\pi}{2} \right]^7 = 0.0014 \approx 0, \quad (\text{A4b})$$

$$C = -\frac{3}{3!} \left[\frac{\pi}{2} \right]^3 + 2 \frac{5}{5!} \left[\frac{\pi}{2} \right]^5 - 3 \frac{7}{7!} \left[\frac{\pi}{2} \right]^7 = -1.2393. \quad (\text{A4c})$$

The confinement energy E is then given by the squared positive solution of Eq. (A3)

$$E \approx \left\{ \frac{\sqrt{E_i}}{2C} (\sqrt{E_i/V} - B) + \left[\frac{E_i}{4C^2} (B - \sqrt{E_i/V})^2 - \frac{A}{C} E_i \right]^{1/2} \right\}^2. \quad (\text{A5})$$

In Fig. 9 we compare, for different values of the quantum-well depth V , our approximation [Eq. (A5)] with the exact values obtained from numerical resolution of Eq. (11). We have used $m = 0.067m_0$, which corresponds to GaAs quantum wells. The agreement is very good for wide wells because in that case $E/E_i \approx 1$, so that

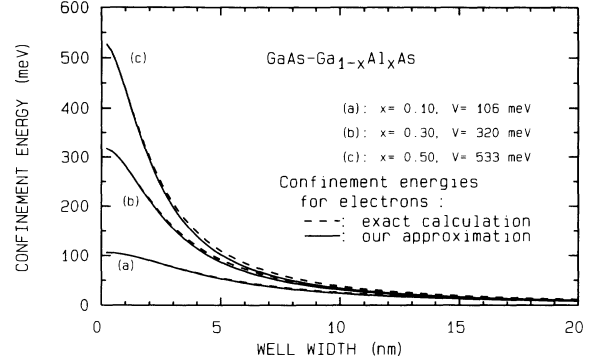


FIG. 9. Electron confinement energy as a function of the well width for a finite quantum well. Comparison of our analytical solution [Eq. (A5)] with the exact numerical resolution of Eq. (11), for different values of the well depth.

the sine-function expansion [Eq. (A2)] is a very good approximation, and for narrow wells because in that case $E/E_i \ll 1$ (E is limited to the value of V) and the expansion of Eq. (A2) becomes very good. The maximum deviations ΔE are 1.7, 5, and 8.3 meV, which occur at $L_w = 86, 50, \text{ and } 38 \text{ \AA}$, for $V = 106, 320, \text{ and } 533 \text{ meV}$, respectively. On account of the good agreement discussed above, Eq. (A5) may be used to obtain, without calculation, a good and rapid estimation of the ground-state energy E_1 in a finite quantum well. With regard to the exciton problem, the agreement of Eq. (A5) with the exact solution is wide enough to be used, and then permits one to propose a full-analytic calculation of the exciton binding energy for ground-state transitions $e1\text{-hh}1$ and $e1\text{-lh}1$.

- ¹R. C. Miller, D. A. Kleinmann, W. T. Tsang, and A. C. Gossard, Phys. Rev. B **24**, 1134 (1981).
²G. Bastard, E. E. Mendez, L. L. Chang, and L. Esaki, Phys. Rev. B **26**, 1974 (1982).
³D. A. B. Miller, D. S. Chemla, T. C. Damen, A. C. Gossard, W. Wiegmann, T. Wood, and C. A. Burrus, Phys. Rev. B **32**, 1043 (1985).
⁴R. L. Greene, K. K. Bajaj, and D. E. Phelps, Phys. Rev. B **29**, 1807 (1984).
⁵G. Priester, G. Allan, and M. Lannoo, Phys. Rev. B **30**, 7302 (1984).
⁶G. D. Sanders and Y. C. Chang, Phys. Rev. B **32**, 5517 (1985).
⁷D. A. Broido and L. J. Sham, Phys. Rev. B **34**, 3917 (1986).
⁸U. Ekenberg and M. Altarelli, Phys. Rev. B **35**, 7585 (1987).
⁹G. E. W. Bauer and T. Ando, Phys. Rev. B **38**, 6015 (1988).
¹⁰J. W. Wu, Phys. Rev. B **39**, 12 944 (1989).
¹¹L. C. Andreani and A. Pasquarello, Phys. Rev. B **42**, 8928 (1990).
¹²R. P. Leavitt and J. W. Little, Phys. Rev. B **42**, 11 774 (1990).
¹³X. F. He, Phys. Rev. B **43**, 2063 (1991).
¹⁴G. Bastard, *Wavemechanics Applied to Semiconductor Hetero-*

- structures* (Les Éditions de Physique, Paris, 1988), p. 250.
¹⁵A. Baldereschi and N. O. Lipari, Phys. Rev. B **3**, 439 (1971).
¹⁶U. Ekenberg, Phys. Rev. B **40**, 7714 (1989).
¹⁷M. Braun and U. Rössler, J. Phys. C **18**, 3365 (1985).
¹⁸D. M. Whittaker and R. J. Elliott, Solid State Commun. **68**, 1 (1988).
¹⁹D. B. Tran Thoai, R. Zimmermann, M. Grundmann, and D. Bimberg, Phys. Rev. B **42**, 5906 (1990); M. Grundmann and D. Bimberg, Phys. Rev. B **38**, 13 486 (1988).
²⁰C. Bosio, J. L. Staehli, M. Guzzi, G. Burri, and R. A. Logan, Phys. Rev. B **38**, 3263 (1988).
²¹P. Dawson, K. J. Moore, G. Duggan, H. I. Ralph, and C. T. B. Foxon, Phys. Rev. B **34**, 6007 (1986).
²²D. C. Reynolds, K. K. Bajaj, C. Leak, G. Peters, W. Theis, P. W. Yu, K. Alavi, C. Colvard, and I. Shidlovsky, Phys. Rev B **37**, 3117 (1988).
²³L. W. Molenkamp, G. E. W. Bauer, R. Eppenga, and C. T. B. Foxon, Phys. Rev. B **38**, 6147 (1988).
²⁴A. Petrou, G. Waytena, X. Liu, J. Ralston, and G. Wicks, Phys. Rev. B **34**, 7436 (1986).
²⁵H. Mathieu, P. Lefebvre, and P. Christol (unpublished).